Electronic Supplementary Material (ESI) for Soft Matter.

Supporting Information

Characterizing Surface Wetting and Interfacial Properties using Enhanced Sampling (SWIPES)

Hao Jiang[†], Suruchi Fialoke [†], Zachariah Vicars [†] and Amish J. Patel[†]

[†] *Department of Chemical and Biomolecular Engineering, University of Pennslyvania, Philadelphia, PA 19104, United States*

1 Location of the observation volume v

The observation volume is chosen to be a cuboid. The left edge of v is placed around 1 nm to the left of the leftmost atoms in the solid surface. As shown in Figure 1 of the main text, the observation volume covers the entire solid surface, and its right edge is placed to the right of the rightmost solid atoms. Out of the two vapor-liquid interfaces that separate the liquid slab and vapor, the left interface remains well outside v (far from the surface), whereas the right interface remains well within v in all of our biased simulations. These choices enable us to ensure that as the liquid slab moves along the surface, the only physical process that occurs is the replacement of vapor-solid interfacial area by an equivalent amount of liquid-solid interfacial area, and that there are no edge effects.

2 Interface position H and free energy F_{κ,N^*} vary linearly with N^*

To show that the interface position $H \equiv \langle x_{\mathrm{COM}} \rangle_{\kappa,N^*}$ and free energy F_{κ,N^*} in the biased ensemble vary linearly with N^*, we first consider an ensemble with a constant number of coarse-grained waters, $\tilde{N}$, in the observation volume, v. The free energy difference between such an ensemble and the unbiased ensemble, $F_v(\tilde{N})$, is related to the statistics, $P_v(\tilde{N}) = \langle \delta(\tilde{N}_v - \tilde{N}) \rangle_0$, of coarse-grained water numbers in v through $\beta F_v(\tilde{N}) = -\ln P_v(\tilde{N})$; here $\langle \mathcal{O}(\overline{\mathbf{R}}) \rangle_0$ represents the average of $\mathcal{O}(\overline{\mathbf{R}})$ in the unbiased ensemble. In the constant-$\tilde{N}$ ensemble, the position of the vapor-liquid interface, H_n, can be characterized using the corresponding ensemble average of the water slab center of mass position in the simulation box in the direction (x) perpendicular to the vapor-liquid interface, i.e., $H_n \equiv \langle x_{\mathrm{COM}} \rangle_{\tilde{N}}$, where $\langle \mathcal{O}(\overline{\mathbf{R}}) \rangle_{\tilde{N}}$ represents the average of $\mathcal{O}(\overline{\mathbf{R}})$ in the constant-$\tilde{N}$ ensemble.

As the number of coarse-grained water molecules inside the observation volume (v) is increased by $\delta\tilde{N}$, the vapor-liquid interface ought to advance along the surface in x-direction by a distance δH_n. However, the shape of the vapor-liquid interface is expected to be independent of $\tilde{N}$; instead, it is determined by the balance of forces at the 3-phase contact line, which is governed entirely by the corresponding interfacial tensions. Thus, $\delta\tilde{N}$ and δH_n ought to be related through:

$$\delta\tilde{N} = \delta H_n \times L \times \int_{z_{\mathrm{low}}}^{z_{\mathrm{high}}} [\tilde{\rho}_{\mathrm{L}}(z) - \tilde{\rho}_{\mathrm{V}}(z)] dz, \tag{1}$$

where $\tilde{\rho}_{\mathrm{L}}(z)$ and $\tilde{\rho}_{\mathrm{V}}(z)$ are the coarse-grained density profiles (along the z-axis) of the liquid and vapor confined between the two solid surfaces, respectively. L is the length of the simulation box along the y-axis, and z_{low} and z_{high} are the lowest and highest coordinates of solid atoms that are in contact with water molecules, respectively. The corresponding slope, $h_n \equiv dH_n/d\tilde{N}$ can then be expressed as:

$$h_n = \frac{1}{L \times \int_{z_{\mathrm{low}}}^{z_{\mathrm{high}}} [\tilde{\rho}_{\mathrm{L}}(z) - \tilde{\rho}_{\mathrm{V}}(z)] dz}. \tag{2}$$

For a homogeneous flat solid surface, the water density profile remains unchanged regardless the position of the interface, and both z_{low} and z_{high} are constants. Therefore, the slope h_n is a constant, i.e. H_n is a linear function of $\tilde{N}$. Because free energy and interface position are linearly related to one another (Equation 3 of the main text), $F_v(\tilde{N})$ should also be a linear function of $\tilde{N}$, making $f_n \equiv dF_v(\tilde{N})/d\tilde{N}$ a constant.

Moreover, the free energetics of the constant-$\tilde{N}$ ensemble, $F_v(\tilde{N})$, and the free energetics of biased ensemble, F_{κ,N^*}, are related through [1,2]

$$F_v(\tilde{N}) = F_v^{\kappa,N^*}(\tilde{N}) - U_{\kappa,N^*}(\tilde{N}) + F_{\kappa,N^*}, \tag{3}$$

where $U_{\kappa,N^*}(\tilde{N}) = \frac{\kappa}{2}(\tilde{N} - N^*)^2$ is the parabolic biasing potential, and $\beta F_v^{\kappa,N^*}(\tilde{N}) = -\ln P_v^{\kappa,N^*}(\tilde{N})$ represents the free energetics of $\tilde{N}_v$ in the biased ensemble, with the corresponding statistics being given by $P_v^{\kappa,N^*}(\tilde{N}) = \langle \delta(\tilde{N}_v - \tilde{N}) \rangle_{\kappa,N^*}$. Taking the derivative of Equation 3 with respect to $\tilde{N}$:

$$f_n \equiv \frac{\partial F_v}{\partial \tilde{N}} = \frac{\partial F_v^{\kappa,N^*}}{\partial \tilde{N}} - \kappa(\tilde{N} - N^*), \tag{4}$$

where as discussed above, f_n is a constant (independent of $\tilde{N}$). By recognizing that $F_v^{\kappa,N^*}(\tilde{N})$ ought to have a minimum at $\tilde{N} = \langle \tilde{N}_v \rangle_{\kappa,N^*}$, and that the corresponding $\tilde{N}$-derivative ought to be 0, we get:

$$f_n = -\kappa[\langle \tilde{N}_v \rangle_{\kappa,N^*} - N^*]. \tag{5}$$

From Equation 6 of the main text, we then see that

$$f_n = \kappa[N^* - \langle \tilde{N}_v \rangle_{\kappa,N^*}] = f. \tag{6}$$

Because f_n is a constant, $f \equiv dF_{\kappa,N^*}/dN^*$ should also be a constant. Thus, F_{κ,N^*} must be a linear function of N^*. Finally, because the free energetics, F_{κ,N^*}, and interface position, $H \equiv \langle x_{\mathrm{COM}} \rangle_{\kappa,N^*}$, in the biased ensemble are linearly related to one another (Equation 3 of the main text), H must also a linear function of N^*, and h a constant.

For the LJ surface with ϵ_{SW}=1.94 kJ/mol, we used umbrella sampling to obtain $F_v(\tilde{N})$; i.e., we employed biased simulations with sufficient overlap in the distributions, $P_v^{\kappa,N^*}(\tilde{N})$, between neighboring windows. We then analyzed the results using standard techniques, such as the weighted histogram analysis algorithm (WHAM)[3] to obtain both $F_v(\tilde{N})$ as a function of $\tilde{N}$, and F_{κ,N^*} as a function of N^*. These results are shown in Figures S1a and S1b, and confirm the linear dependences of $F_v(\tilde{N})$ on $\tilde{N}$ and of F_{κ,N^*} on N^*; the corresponding slopes, f and f_n also agree with one another, as expected. The simple (linear) dependences of $F_v(N)$ and F_{κ,N^*} as well as of H_n and H makes the estimation of f and h both straightforward and efficient, and lie at the heart of the simplicity and computational efficiency of SWIPES.

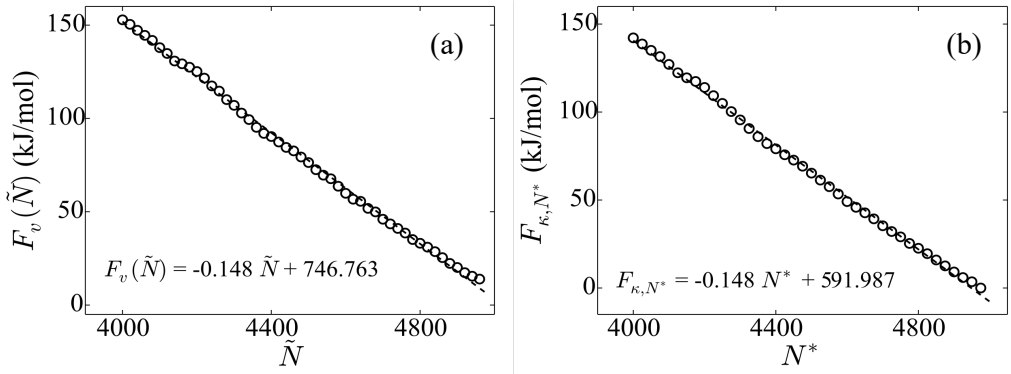

Figure S 1: For the LJ surface with $\epsilon_{\mathrm{SW}} = 1.94$ kJ/mol: (a) $F_v(\tilde{N})$ calculated using umbrella sampling and WHAM (black symbols) is shown as a function of $\tilde{N}$. (b) F_{κ,N^*} calculated using umbrella sampling and WHAM (black symbols) is shown as a function of N^*. The dashed lines are linear fits to the data.

3 Estimating f from individual biased simulations

By using Equation 7 of the main text, f can be estimated from every biased simulation. Such estimates are shown in Figure S2 (symbols) for the LJ surface with $\epsilon_{\mathrm{SW}} = 1.94$ kJ/mol. The average of

f over the 12 independent simulations is indicated by the horizontal dashed line, and is in agreement with f calculated from the y-intercept of $\langle N_v \rangle_{\kappa,N^*}$ vs N^*; see Figure 2a of the main text.

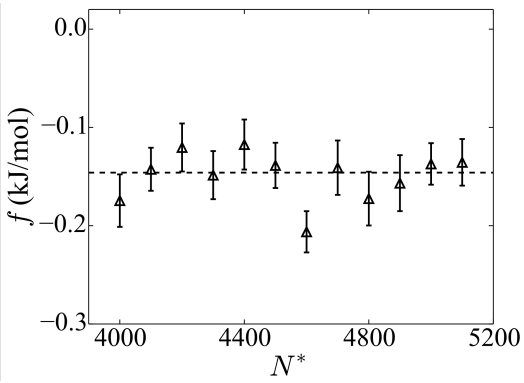

Figure S 2: For the LJ surface with $\epsilon_{\rm SW} = 1.94$ kJ/mol, $f = \kappa(N^* - \langle \tilde{N}_v \rangle_{\kappa,N^*})$ (Equation 7 of the main text) is estimated from each biased simulation (symbols). The horizontal dashed line is the value of f averaged over the 12 f-estimates obtained from the biased simulations.

4 Estimating h from covariances

From every biased simulation, the slope, $h \equiv d\langle x_{\rm COM} \rangle_{\kappa,N^*}/dN^*$ can be estimated using the co-variance of the fluctuations in $x_{\rm COM}$ and $\tilde{N}_v$ (Equation 9 of the main text). For the LJ surface with $\epsilon_{\rm SW} = 1.94$ kJ/mol, h thus obtained is shown as a function of N^* in Figure S3; it is clear that the statistical uncertainties associated with the corresponding estimates of h is substantial. The average of the h-estimates obtained using the co-variance relation from the 12 biased simulations is $7.8(\pm 1) \times 10^{-4}$ nm (dashed line in Figure S3), and agrees reasonably well with the estimate of h obtained from the slope of the line fitted to $\langle x_{\rm COM} \rangle_{\kappa,N^*}$ vs N^* (Figure 2b of the main text).

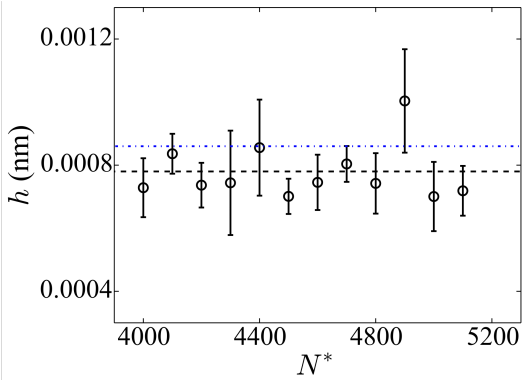

Figure S 3: For the LJ surface with $\epsilon_{\rm SW} = 1.94$ kJ/mol, h estimated from the co-variance of $x_{\rm COM}$ and $\tilde{N}_v$ is shown for each biased simulation (symbols). The dashed line (black) indicates the average of the 12 h-estimates obtained from the biased simulations. The dot-dashed line (blue) indicates the value of h obtained in Figure 2b of the main text.

5 $\langle \tilde{N}_v \rangle_{\kappa,N^*}$ and $\langle x_{COM} \rangle_{\kappa,N^*}$ for LJ surfaces with different ϵ_{SW}-values

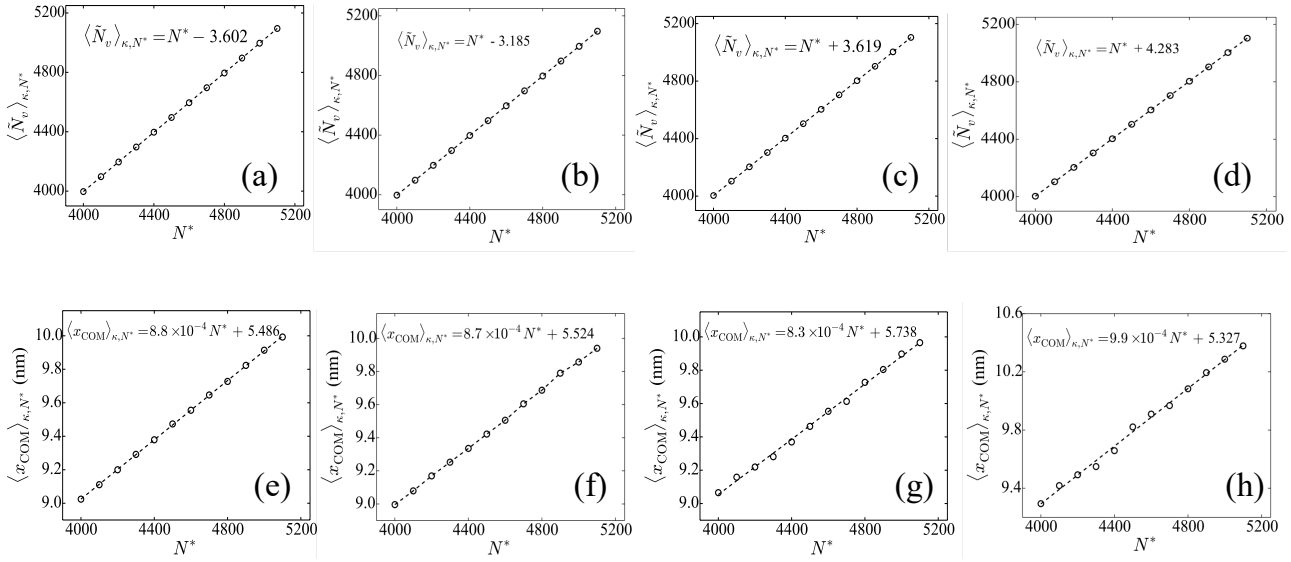

Figure S 4: Ensemble averages of the coarse-grained number of water in the observation volume, $\langle \tilde{N}_v \rangle_{\kappa,N^*}$, are shown as a function of N^* for LJ surfaces with ϵ_{SW}-values of (a) 0.1 kJ/mol, (b) 0.5 kJ/mol, (c) 2.08 kJ/mol, and (d) 2.25 kJ/mol, respectively. Ensemble averages of water slab center of mass position along the x-axis, $\langle x_{\mathrm{COM}} \rangle_{\kappa,N^*}$, are shown as a function of N^* for LJ surface with ϵ_{SW}-values of (e) 0.1 kJ/mol, (f) 0.5 kJ/mol, (g) 2.08 kJ/mol, and (h) 2.25 kJ/mol, respectively. Dashed lines are linear fits to the simulation data (symbols). In fitting $\langle \tilde{N}_v \rangle_{\kappa,N^*}$ vs. N^*, the slope is set to 1.

6 Effect of solid surfaces separation distance on the calculation of k

For all the biased simulations described in the main text, the length of the simulation box in the z-direction, L_z, (which sets the separation between the solid surface) was fixed to be 14.319 nm. Here we estimate k using a smaller and larger systems with L_z-values of 10.023 nm and 17.182 nm, respectively. While 7000 water molecules were used in the biased simulations reported in the main text, 5000 and 12000 waters are used in the small and large systems, respectively. The solid surfaces themselves continue to be made up from 8640 atoms. In Figure S5, the ensemble averages $\langle \tilde{N}_v \rangle_{\kappa,N^*}$ and $\langle x_{\mathrm{COM}} \rangle_{\kappa,N^*}$ are shown as functions of N^* for the small and large systems, and enable estimation of k. The contact angles thus estimated from the small and large systems using SWIPES are 40(2)° and 41(2)°, respectively, and agree with one another as well as with the system used in the main text within statistical uncertainty. Alternatively, contact angles can also be extracted from vapor-liquid interface geometries, as shown in Figure S6. The contact angles thus estimated for the small and large systems are 38(3)° and 39(3)°, respectively, and agree with one another as well as with the system used in the main text within statistical uncertainty.

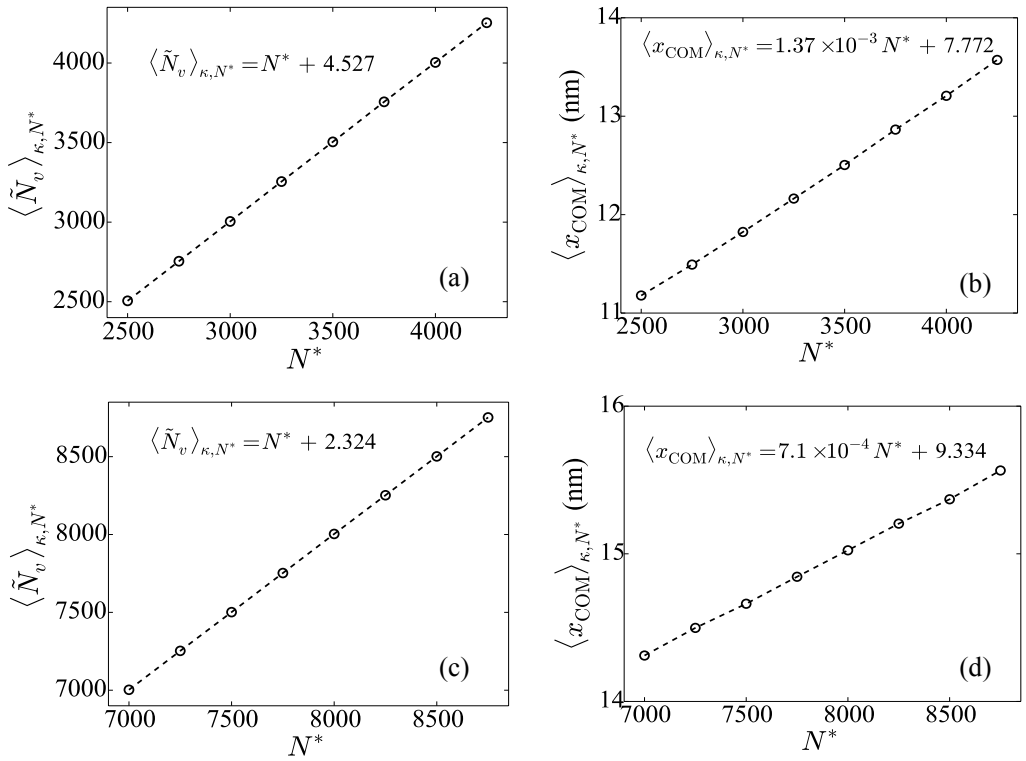

Figure S 5: For the LJ surface with $\epsilon_{\mathrm{SW}} = 1.94$ kJ/mol: (a) Ensemble average of the coarse-grained number of waters in the observation volume, $\langle \tilde{N}_v \rangle_{\kappa,N^*}$, as a function of N^* obtained from biased simulations using the small system (see text). (b) Ensemble average of water slab center of mass position along the x-axis, $\langle x_{\mathrm{COM}} \rangle_{\kappa,N^*}$, as a function of N^* obtained from biased simulations using the small system. (c) Ensemble average of the coarse-grained number of water in the observation volume, $\langle \tilde{N}_v \rangle_{\kappa,N^*}$, as a function of N^* obtained from biased simulations using the large system (see text). (d) Ensemble average of water slab center of mass position along the x-axis, $\langle x_{\mathrm{COM}} \rangle_{\kappa,N^*}$, as a function of N^* obtained from biased simulations using the large system.

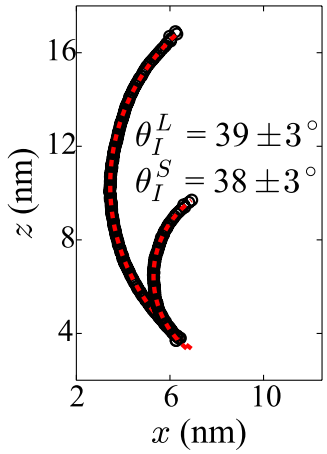

Figure S 6: Vapor-liquid interface profiles for the LJ surface with ϵ_{SW} =1.94 kJ/mol obtained from biased simulations of the large (L) and small (S) systems; the interface profiles are fit to circles (red dashed lines).

7 Geometry of vapor-liquid interfaces

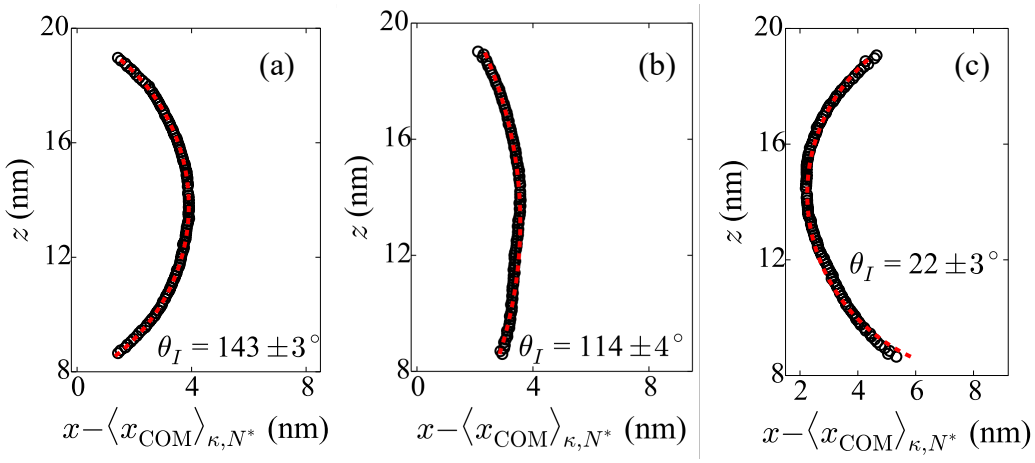

Figure S 7: Vapor-liquid interface profiles obtained from our biased simulations for LJ surfaces with ϵ_{SW} of (a) 0.5 kJ/mol, (b) 1.0 kJ/mol, and (c) 2.02 kJ/mol, respectively; the profiles are fit to circles (red dashed lines).

8 Geometry of cylindrical droplets

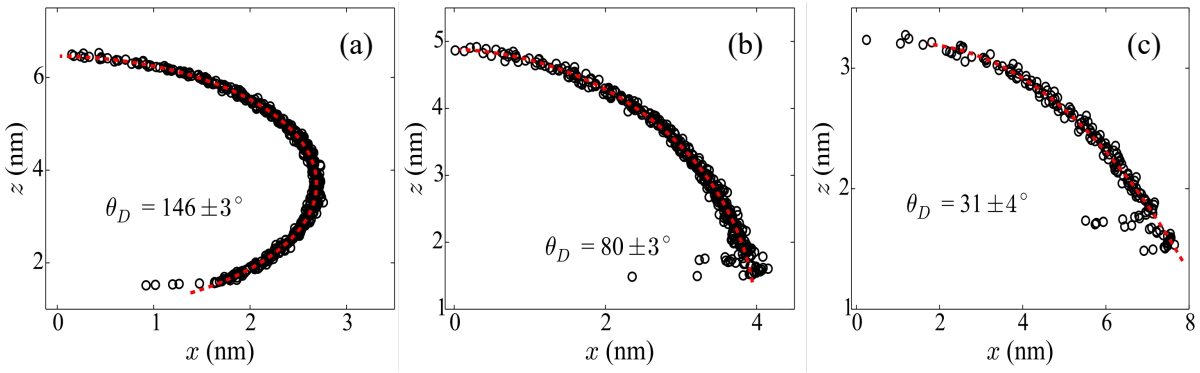

Figure S 8: Vapor-liquid interface profiles for cylindrical water droplets on LJ surfaces with ϵ_{SW} of (a) 0.5 kJ/mol, (b) 1.5 kJ/mol, and (c) 2.02 kJ/mol, respectively; the profiles are fit to circles (red dashed lines).

References

[1] E. Xi, R. C. Remsing and A. J. Patel, *J. Chem. Theory Comput.*, 2016, **12**, 706–713.

[2] E. Xi, S. M. Marks, S. Fialoke and A. J. Patel, *Mol. Simul*, 2018, **44**, 1124–1135.

[3] M. Souaille and B. Roux, *Comput. Phys. Commun.*, 2001, **135**, 40–57.